Rhodium-Catalyzed Hydrocarboxylation: Mechanistic Analysis Reveals Unusual Transition State for Carbon-Carbon Bond Formation

Ljiljana Pavlovic,[&] Janakiram Vaitla,[#] Annette Bayer,[#] Kathrin H. Hopmann[&*]

[#]Department of Chemistry, University of Tromsø -The Arctic University of Norway, N-9037 Tromsø, Norway

[&]Hylleraas Centre for Quantum Molecular Sciences, Department of Chemistry, University of Tromsø - The Arctic University of Norway, N-9037 Tromsø, Norway

Supporting Information Placeholder

ABSTRACT: The mechanism of rhodium-COD-catalyzed hydrocarboxylation of styrene-derivatives and α,β-unsaturated carbonyl compounds with CO_2 has been investigated using density functional theory (PBE-D2/IEFPCM). The calculations support a catalytic cycle as originally proposed by Mikami and coworkers including β-hydride elimination, insertion of the unsaturated substrate into a rhodium-hydride bond and subsequent carboxylation with CO_2. The CO_2 insertion step is found to be rate-limiting. The calculations reveal two interesting aspects: Firstly, during C-CO_2 bond formation, the CO_2 molecule interacts with neither the rhodium complex nor the organozinc additive. This appears to be in contrast to other CO_2 insertion reactions, where CO_2-metal interactions have been predicted. Secondly, the substrates show an unusual coordination mode during CO_2 insertion, with the nucleophilic carbon positioned up to 3.6 Å away from rhodium. In order to understand the experimentally observed substrate preferences, we have analyzed a set of five alkenes: an α,β-unsaturated ester, an α,β-unsaturated amide, styrene and two styrene-derivatives. The computational results and additional experiments reported here indicate that the lack of activity with amides is caused by a too high barrier for CO_2 insertion and is not due to catalyst inactivation. Our experimental studies also reveal two putative side reactions, involving oxidative cleavage or dimerization of the alkene substrate. In the presence of CO_2, these alternative reaction pathways are suppressed. The overall insights may be relevant for the design of future hydrocarboxylation catalysts.

INTRODCUTION

Hydrocarboxylation of alkenes is a promising strategy for formation of alkyl carboxylic acids from CO_2. In 2008, Rovis and coworkers reported seminal studies on nickel-catalyzed hydrocarboxylation of alkenes with CO_2.[1] Subsequently, related reactions have been communicated involving different catalysts based on Cu/Fe,[2] Fe,[3] Ti,[4] Rh[5] or Ru[6].

The reaction mechanisms of metal-catalyzed hydrocarboxylation of different types of unsaturated substrates have been addressed computationally (for a relevant review see ref. 7). A small number of studies have investigated hydrocarboxylation of alkene substrates with CO_2.[8,9,10] Despite large differences in catalysts, the different alkene hydrocarboxylation reactions have been proposed to follow similar patterns, involving formation of a metal-hydride (e.g. through β-hydride elimination from a transmetallated alkyl ligand), insertion of the alkene substrate into the metal-hydride bond to form a metal-alkyl species and subsequent reaction with CO_2 to yield the carboxylic acid (**Figure 1A**).[3,5,8,9,10] Variations of this mechanism are seen, e.g. for a Fe-pincer complex with EtMgBr as additive, it has been proposed that an explicit Fe-hydride might not be formed, but that the transmetallated ethyl-ligand could donate a hydride directly to the styrene substrate.[8] A computational investigation of a hypothetical reaction involving Rh-pincer complexes explored the potential of H_2 as hydride donor, but the study showed that this might lead to a competing hydrogenation reaction.[9] Theoretical studies of a Ni-$(DBU)_2$ complex with $ZnEt_2$ as additive concluded that formation of a Ni-hydride complex might compete with oxidative coupling of the alkene substrate and CO_2 to form a low-lying metallacycle.[10]

Related reactions involving insertion of CO_2 into metal-alkyl bonds have also been studied computationally, including cop-

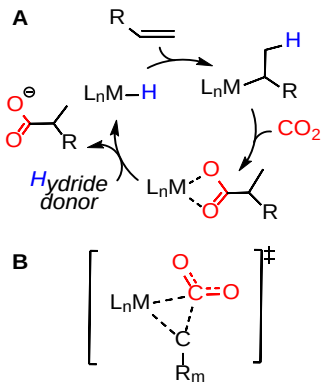

CO_2 insertion TS

Figure 1. A) Generalized mechanism for hydrocarboxylation of alkenes with CO_2 (transmetallation steps not shown, based on [3,5,8,9,10]). **B**) Proposed conformation of C-CO_2 bond formation TS for reactions involving Ni,[10, 11, 16, 17, 20] Cu,[12,13,14] Rh,[9,21,22] or Fe/Mg.[8]

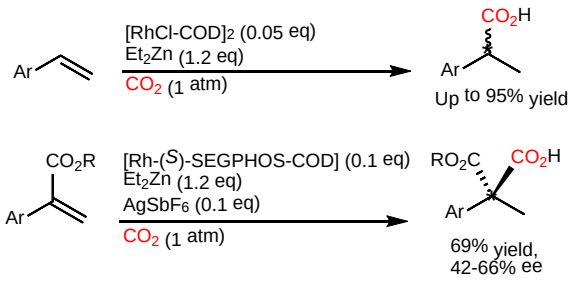

Figure 2. Rhodium-catalyzed hydrocarboxylation of alkenes with CO_2, as reported by Mikami and coworkers.[5]

per-catalyzed carboxylation of alkynes[13,14] or organoboranes,[15] nickel-catalyzed carboxylation of aryl or benzyl halides,[16,17] or coupling of CO_2 with ethylene,[18,19] or acetylene,[20] and insertion of CO_2 into rhodium-ethyl or aryl bonds.[21,22,24] Despite the molecular differences of these systems, the carbon-CO_2 bond formation step is expected to occur in a similar fashion via a three-membered transition state (TS), where CO_2 is predicted to interact with the metal via the carbon atom or through an η^2-C,O coordination mode (**Figure 1B**, for a recent review see 23).[8,9,10,11,12,13,14,20,21,22,24] An exception is CO_2 insertion into nickel-methyl or -allyl bonds, for which it has been predicted that CO_2 has no interaction with the metal centre during the C-CO_2 bond formation step.[25]

Several of the reported hydrocarboxylation reactions of alkenes result in the formation of chiral carboxylic acids, but racemic mixtures are obtained due to the use of symmetric catalysts.[1,3,4] To date, only one asymmetric CO_2-based hydrocarboxylation reaction has been reported, involving a rhodium complex with a bidentate SEGPHOS ligand, which in presence of $ZnEt_2$ carboxylates α,β-unsaturated esters with up to 66 % enantiomeric excess *ee* (**Figure 2**).[5] The hydrocarboxylation activity of rhodium catalysts with bidentate ligands appears to be highly dependent on both the nature of the ligand and the properties of the substrate.[5] With Rh-COD, α,β-unsaturated esters and styrene-derivatives with electron-withdrawing *para*-substituents are converted with reasonable yields, however, α,β-unsaturated amides and styrene itself are completely unreactive.[5]

Detailed insights into the reaction mechanism may be valuable for improving the activity, substrate scope and selectivity of rhodium-catalyzed hydrocarboxylation reactions. Here we have studied the mechanism of rhodium-COD/$ZnEt_2$-mediated alkene hydrocarboxylation using DFT methods on the full molecular system. Besides the mechanistic details, our aim was to elucidate the substrate preferences of this reaction, and to understand how CO_2 and the substrate interact with the rhodium complex. Our theoretical analysis reveal two interesting aspects: Firstly, during C-CO_2 bond formation, the CO_2 molecule interacts with neither the rhodium complex nor the organozinc additive. This is in contrast to most previous computational studies, which predict a metal-CO_2 interaction (**Figure 1**).[8,9,10,11,12,13,14,20,21,22,24] Secondly, in the C-C bond forming step, the substrates prefer an η^6-coordination mode to rhodium, with the nucleophilic carbon positioned several Å away from the metal centre. Although η^6-binding modes are well-known for coordination of ligands,[26,27,28,29] to our knowledge such a binding mode has not previously been predicted to occur during conversion of styrene-type substrates. In order to understand the experimental substrate preferences, we have analysed a set of five substrates and show that the proposed mechanism can explain why esters are the preferred substrates, whereas amides are unreactive. We further report experimental studies that reveal two putative side reactions, which appear to be suppressed in presence of CO_2.

METHODS:

Computational models: All calculations were performed with the full catalyst and full substrates (**Figure 3**), without truncations or symmetry constraints, and with a closed-shell spin state. The effect of the solvent was modelled through inclusion of the polarizable continuum solvent model IEFPCM (dimethylformamide, which is the solvent employed in experiments[5]) in geometry optimizations and energy evaluations.

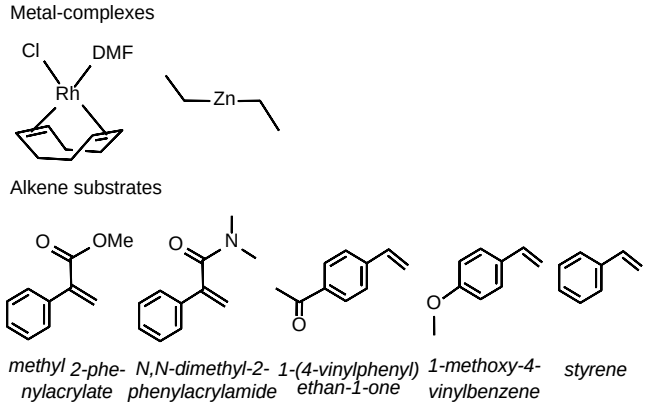

Figure 3. Metal complexes and substrates studied here.

Computational methods: All calculations were performed with Gaussian 09, Rev. D01[30]. The DFT functional PBEPBE[31], including both the Grimme empirical dispersion correction (D2[32]) and IEFCPM[33] (solvent = *n*,*n*-dimethylformamide) were employed in all calculations. We have previously shown that this computational protocol provides good accuracies.[34] In geometry optimizations, the basis set 6-311G(d,p) was employed on all non-metal atoms and zinc, whereas Lanl2DZ (including pseudopotential) was employed on rhodium, including an extra f-polarization function with exponent 1.35[35] (this basis set combination is here referred to as BS1). Big basis set single-point corrections to the energies where computed employing 6-311+G(2d,2p) on all non-metal atoms and zinc, while Lanl2TZ(f) was used for rhodium (referred to as BS2). Counter poise corrections (CP) were computed with BS2 to estimate the magnitude of the basis set super position error when joining several molecules into one model.[36] The CP corrections were found to be small and they were not included in the final energies.

The thermodynamic parameters were obtained from frequency calculations and were corrected to the experimental temperature of 273 K. In order to convert computed free energies ($\Delta G°_{1atm,BS1}$) from a 1 atm to a 1 M standard state, a standard state conversion factor (SS) was included, which can be calculated as $R_1 T \ln(R_2 T^{\Delta n})$, where R_1 = 8.31447 J K^{-1} mol^{-1}, R_2 = 0.08206 L atm K^{-1} mol^{-1}, T = temperature in K, and Δn = change in number of moles.[34,37] For an association reaction A+B→C; the change of mole is Δn = -1 and the above expression becomes -1.89 kcal/mol at 298K (-1.69 kcal/mol at 273 K). Unless explicitly stated otherwise, reported energies correspond to solution standard state Gibbs free energies at 273 K ($\Delta G°_{1M,273K}$), including big basis set corrections to the electronic energy (E) and standard state corrections (SS): $\Delta G°_{1M,273K} = \Delta G°_{1atm,BS1,273K} - \Delta E_{BS1} + \Delta E_{BS2} + SS_{273K}$

Experimental details: Diethylzinc (1.0 M in hexane solution) and $[RhCl(cod)]_2$ were purchased from Aldrich. Methyl 2-phenylacrylate and *N*,*N*-diethyl-2-phenylacrylamide were prepared according to the literature.[5] DMF was dried over 4Å molecular sieves. Conversions were monitored by thin-layer chromatography (TLC) with Merck pre-coated silica gel plates (60 F254). Visualization was accomplished with either UV light or by immersion in potassium permanganate or 5% alcoholic phosphomolybdic acid (PMA) followed by light heating with a heating gun. High-resolution mass spectra (HRMS) were recorded from MeOH solutions on an LTQ Orbitrap XL (Thermo Scientific) in positive electrospray ionization (ESI) mode. The mechanistic cycle was studied with methyl 2-phenylacrylate as substrate using stoichiometric catalyst/substrate mixtures, monitored by NMR (for further details, see the Supporting Information, SI).

RESULTS AND DISCUSSION

Mechanistic investigation

The mechanism for rhodium-catalyzed hydrocarboxylation as proposed by Mikami and coworkers[5] is shown in **Figure 4**, with minor modification based on our results. The active rhodium-hydride species is generated in two steps. The first step involves transmetallation of an ethyl group from diethyl-zinc to the precatalyst. This leads to formation of a Rh-Et species, which we predict may loosely coordinate a DMF solvent molecule to form Rh(DMF)Et. The complex then looses DMF and undergoes β-hydride elimination to give a Rh-H species. Next, insertion of the alkene substrate into the Rh-H bond takes place to produce a Rh-Alkyl intermediate.[38] Two possible pathways for alkene insertion exist due to the asymmetry of the double bond. Insertion of CO_2 into the Rh-Alkyl species gives the carboxylated rhodium complex. Finally, transmetallation with diethyl-zinc forms a zinc carboxylate, with simultaneous regeneration of the Rh-Et species. Upon acidic work-up, zinc carboxylate is protonated to provide the α-aryl carboxylic acid.

The computed energy profile is shown in **Figure 5,** with the Rh(DMF)Et species used as an energetic reference. We have used the α,β-unsaturated ester, methyl 2-phenylacrylate, in our

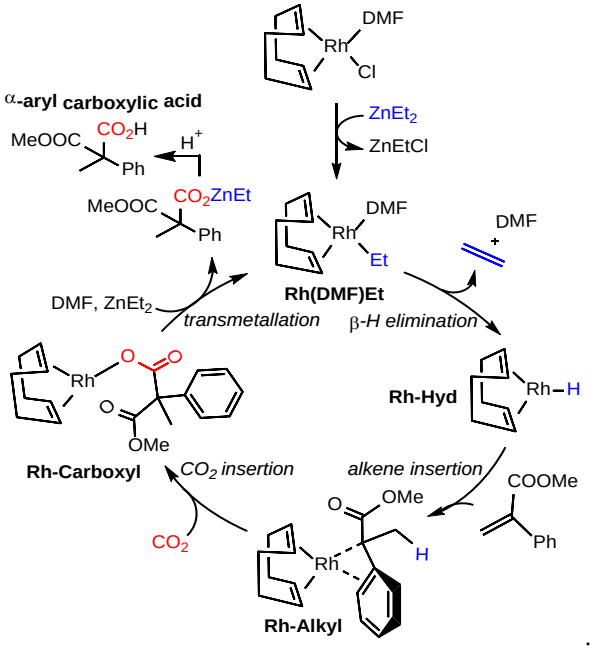

Figure 4. Mechanism for Rh-COD-catalyzed hydrocarboxylation, based on the previous proposal, [5] and computations performed here.

calculations of the full reaction cycle. The first step, β-H elimination, occurs via a four–membered TS ($TS_{β\text{-}Hyd}$) with an activation barrier of 6,8 kcal/mol. The subsequent low-barrier hydride

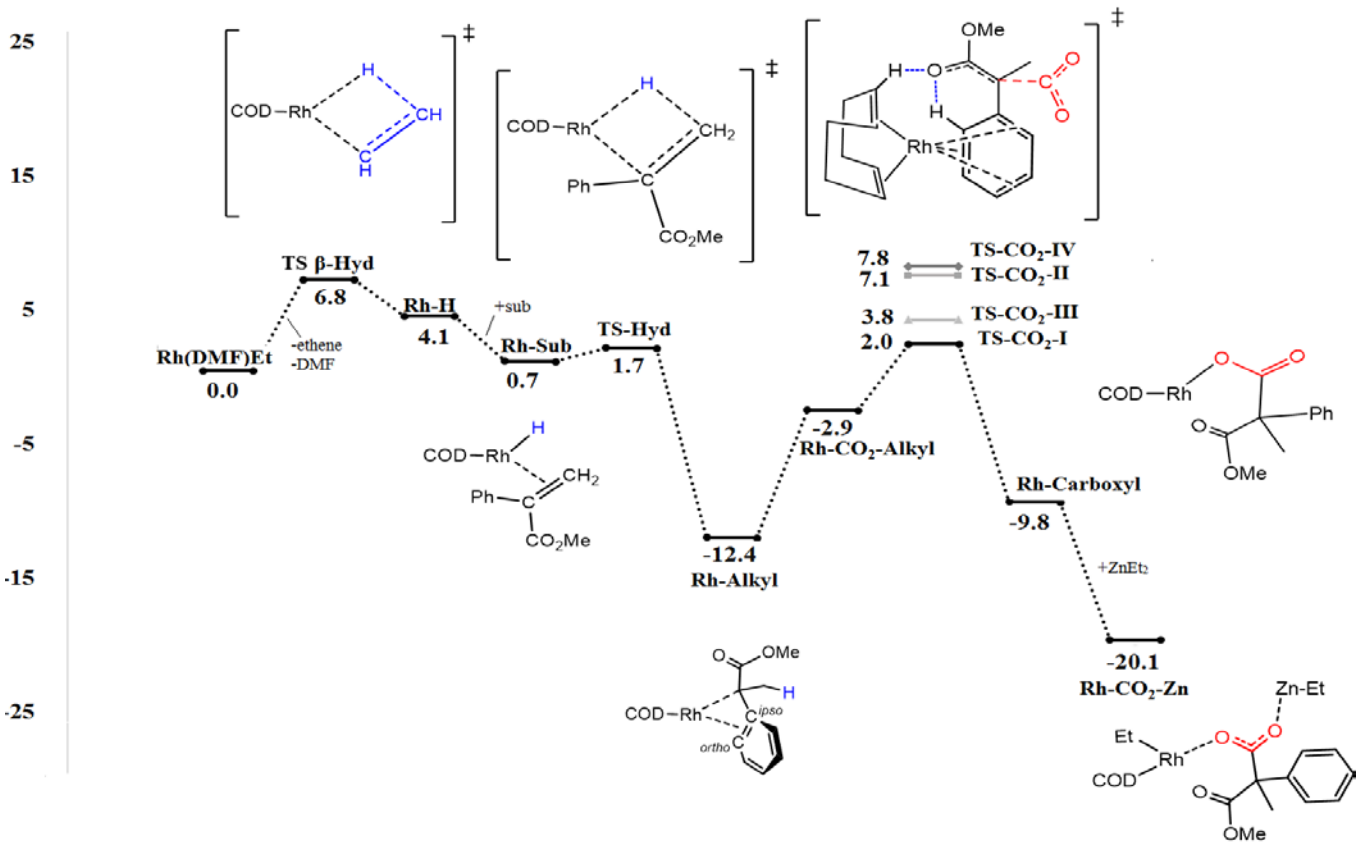

Figure 5. Computed free energy profile (kcal/mol, 273 K, PBE-D2/BS2[IEFPCM]//PBE-D2/BS1[IEFPCM] level of theory) for rhodium-COD catalyzed hydrocarboxylation of methyl 2-phenylacrylate.

transfer to the terminal carbon of the substrate agrees with the experimentally observed product, α-aryl carboxylic acid.[5] The alternative hydride transfer pathway leading to the β-aryl carboxylic acid is higher in energy (SI, Figure S1).

Our calculations indicate that the Rh-Alkyl intermediate formed after substrate insertion is energetically very stable, 12.4 kcal/mol below the Rh(DMF)Et species (**Figure 5**). The optimized geometry of Rh-Alkyl reveals an η^2-coordination mode of the phenyl ring to the metal (**Figure 6A**). This type of interaction is well known and described in the literature.[39] The Rh-C_{ipso} and Rh-C_{ortho} distances are 2.26 Å and 2.27 Å, respectively. We propose that several resonance structures contribute to this binding mode (SI, Figure S2). An alternative binding mode involving the ester moiety was found to be higher in energy by 3.1 kcal/mol (see SI, Figure S3).

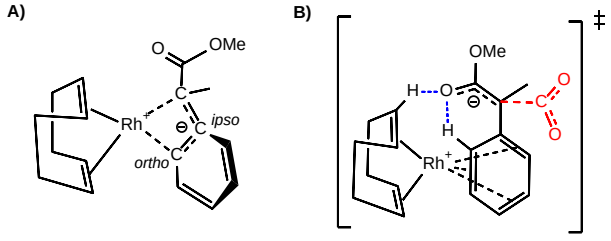

Figure 6. Schematic representation of the energetically preferred conformations of **A**) the Rh-alkyl intermediate, displaying an η^2-coordination mode of the ester and **B**) the TS for CO_2 insertion

($TS_{\_CO2\_I}$), displaying an η^6-coordination of the substrate, with additional CH…O interactions.

In the next step, insertion of CO_2 occurs to give a carboxylated rhodium complex, with a barrier of 14.4 kcal/mol relative to the Rh-Alkyl species ($TS_{CO2\ I}$, **Figure 5**). The carbon-carbon bond formation TS reveals an unusual binding mode of the substrate, with the phenyl ring coordinated to rhodium in an η^6-fashion, whereas the nucleophilic carbon is positioned 3.6 Å away from the metal centre (**Figure 6B** and **7A**). Five of the Rh-C_{phenyl} distances are between 2.24 and 2.37 Å. We predict that the negative charge on the substrate is delocalized over the nucleophilic carbon and the ester oxygen, which is stabilized by two CH…O interactions (distances 2.14 Å and 2.45 Å, respectively, **Figure 6B**). Note that for substrates lacking an adjacent carbonyl, different resonance structures are predicted, with charge delocalization over seven carbon atoms (SI, Figure S4). We optimized an alternative TS geometry, where the carbonyl group of the ester interacts with the metal (TS_{CO2_II},, O...RH distance of 2.16 Å, **Figure 7B**), but this is 1.8 kcal/mol higher in energy compared to $TS_{\_CO2\_I}$. Interestingly, both these TSs show no interaction of the CO_2 molecule with rhodium. If CO_2 is placed closer to rhodium (TS_{CO2_III} and TS_{CO2_IV}, SI, Figure S5), the barrier increases by 5 to 6 kcal/mol, whereas if CO_2 is bound to rhodium in an η^2-fashion (TS_{CO2_V}, SI, Figure S6), the barrier is 23.5 kcal/mol above TS_CO2_I.

We also tested if CO_2 might prefer to interact with the organozinc additive (in analogy to the results by Yuan and coworkers, who proposed that interactions between zinc and CO_2

may take place[10]). However, the optimized geometry of the C-C bond formation TS in presence of $ZnEt_2$ does not indicate that a CO_2-Zn interaction occurs (see SI, Figure S7). This is in line with results by Lv *et al.*,[24] who concluded that an interaction of CO_2 with zinc is energetically disfavored.

The computed energies (**Figure 5**) indicate that insertion of CO_2 may be rate-determining. The carboxylic acid is subsequently transmetallated to zinc and the active rhodium-species is regenerated. A TS for the transmetallation step could not be located, but we do not expect this step to be ratelimiting, as shown by Lv *et al.* for a related Rh-catayzed carboxylation reaction.[24] We optimized an Rh-CO_2-Zn intermediate, where both metals, Rh and Zn, interact with the carboxyl group. The computed energy is -20.1 kcal/mol below the Rh-DMF-ethyl species (**Figure 5**, for the optimized geometry, see SI, Figure S8).

We also performed computations on an alternative reaction pathway, involving formation of a metallacycle from CO_2, alkene, and the rhodium-complex. This was tested in analogy to the results reported for nickel-catalyzed hydrocarboxylation, where a low–lying metallacycle was observed in calculations.[10] However, a rhodacycle intermediate was here found to be higher in energy and was excluded (see SI, Figure S9).

A) TS_{CO2_I}

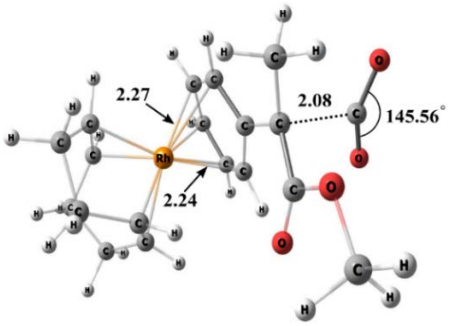

B) TS_{CO2_II}

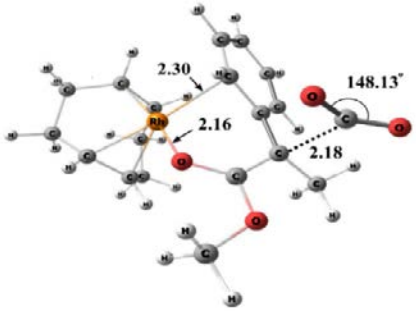

Figure 7. Optimized geometries with methyl 2-phenylacrylate of **A)** the preferred CO_2 insertion TS with η^6-coordination (**TS_{CO_I}**) and **B)** an energetically higher-lying CO_2 insertion TS displaying a Rh-OC_{ester} interaction (**TS_{CO2_II}**). Distances are in Angstrom.

We extended our analysis by additionally performing experimental studies (SI, Figure S10-S14) to shed further light on the catalytic steps of the hydrocarboxylation reaction. When treating $[RhCl(cod)]_2$ (1 equiv.) with Et_2Zn (1 equiv.) in DMF-D_7 in an NMR tube at 0 °C, an immediate color change from pale yellow to dark red was observed. The ^1H NMR spectrum indicated formation of Rh–H species with a diagnostic resonance at -11.74 ppm (**Figure 8**).[40] Then, 2.5 equivalent of methyl 2-phenylacrylate was added to the NMR tube and the resulting complex was characterized. Absence of the olefinic protons of methyl 2-phenylacrylate with chemical shift at 6.37 ppm and 5.90 ppm and the Rh–H chemical shift at -11.74 ppm indicates that insertion of the alkene into the rhodium-hydride took place. However, subsequent bubbling of CO_2 into the NMR tube (for 10 min) did not give the carboxylated product. To investigate the failure of the expected carboxylation step, we analyzed the reaction mixture by HRMS and GCMS prior to CO_2 bubbling. The results indicate formation of a complex reaction mixture including dimerized methyl 2-phenylacrylate and methyl benzoylformate (**Figure 9**).

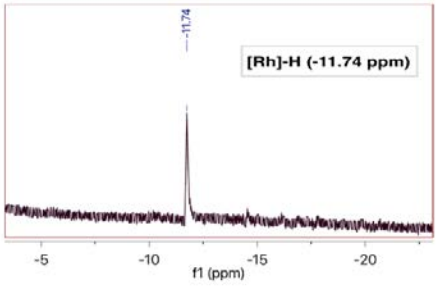

Figure 8. ^1H NMR of [Rh]-H peak

The rhodium-catalyzed alkene dimerization is not a surprising observation,[41] and supports the formation of a rhodium-alkyl intermediate (for mechanistic hypothesis, see SI, Figure S15). Formation of methyl benzoylformate can be explained with a side reaction of the rhodium-complex with O_2 (from air) to generate a Rh(cod)(peroxo) complex, which can further react with alkene to give methyl benzoylformate.[42] To support our hypothesis and confirm the formation of methyl benzoylformate, we carried out the same reaction using 2 mol% of $[RhCl(cod)]_2$ and 1.2 equivalent of $ZnMe_2$ in the presence of air, which gave methyl benzoylformate in 52% yield (for mechanistic hypothesis, see SI, Figure S15). Under ordinary reaction conditions, where a CO_2 atmosphere is present from the initiation of the reaction, the side products discussed here are not formed, and instead methyl 2-phenylacrylate provides 99% yield of the expected carboxylated product.[5] Therefore, we speculate that under reaction conditions, CO_2 inhibits both the formation of the rhodium-peroxo complex (due to reduced presence of O_2) and prevents dimerization of the alkene by promot-

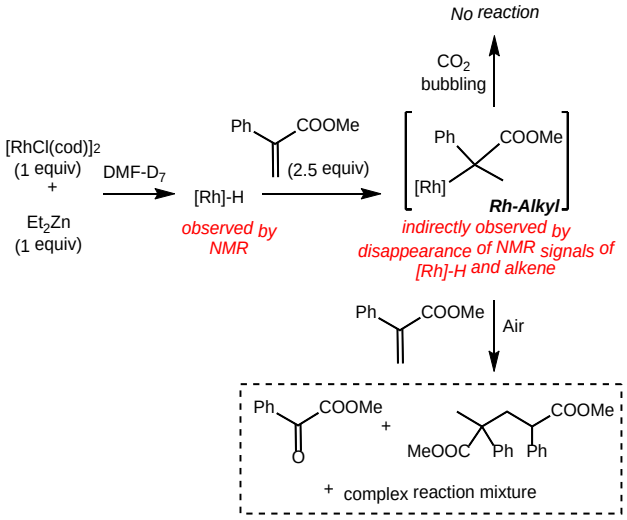

Figure 9. Stoichiometric NMR experiments providing evidence of reaction intermediates as well as side reactions.

substrates bind weaker, but still considerably stronger than the solvent DMF. A correlation between binding strengths and experimental conversions is not evident.

We then performed an experimental test, where we hydrocarboxylated a 1:1 mixture of amide and ester (**Figure 11**). The ester showed full conversion, whereas the amide was unreactive. This confirms that the amide is not inactivating the catalyst. On basis of these results, hypothesis **a** was excluded.

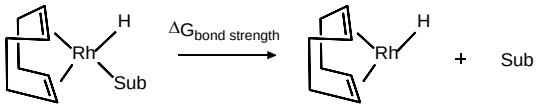

Figure 10. Computation of Rh-substrate bond strength.

Table 1. Computed binding energies and CO_2 insertion barriers for different substrates

Substrate/Ligand	Computed energy for binding to rhodium ($\Delta G_{\text{bond strength}}$ kcal/mol, 298 K)[a]	Computed barrier for CO_2 insertion (relative to Rh-Alkyl-intermediate)[b]	Experimental Yield [%][b]
DMF	-7.1	-	-
Methyl 2-phenylacrylate	-20.9	14.4	>99%
1-methoxy-4-vinylbenzene	-15.9	16.4	0 %
Styrene	-17.3	16.7	0 %
1-(4-vinylphenyl)ethan-1-one	-17.2	18.7	89 %
N,*N*-dimethyl-2-phenylacrylamide	-17.3	19.8	0 %

a) See Fig. 10. Energies at the PBE/BS1(IEFPCM) level. b) From ref. 5 except for the amide, which was studied here, see SI, Fig. S10.

ing carboxylation of the rhodium-alkyl intermediate instead. Our analysis thus points to a serendipitous role of CO_2 in suppressing putative side reactions.

Investigation of the substrate selectivity

In order to understand the experimental substrate preferences, we have performed computational and experimental studies of five substrates: an α,β-unsaturated ester and amide, styrene and two para-substituted styrene-derivatives (**Figure 3**). For two of these substrates, the ester and the para-acetyl styrene, Mikami and coworkers reported yields of 89 to >99% in the Rh-COD-catalyzed hydrocarboxylations whereas the styrene and para-methoxy styrene gave 0% yield.[5] Our experimental results (see SI, Figure S10) are in agreement with earlier results, showing good conversion for the α,β-unsaturated ester and the methyl 2-phenylacrylate. No reaction was detected for an *N*,*N*-diethyl-substituted amide, in agreement with Mikami's studies on a related amide.[5]

We evaluated two hypotheses for the lack of activity of certain substrates: **a**) lack of reactivity is due to substrate-mediated catalyst inactivation, or **b**) lack of reactivity is due to a too high barrier for CO_2 insertion. To evaluate hypothesis **a**, we computed the energies ($\Delta G_{\text{bond strength}}$) for binding the five substrates or a solvent molecule to rhodium (**Table 1**, **Figure 10**). The ester has the strongest binding energy (-20.9 kcal/mol). The other

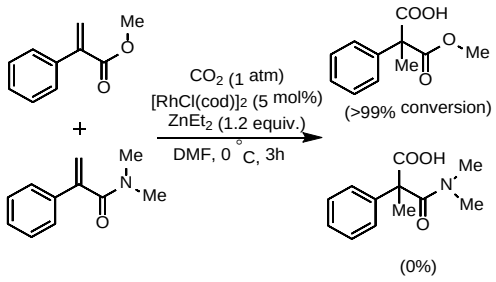

Figure 11. Rh-catalyzed hydrocarboxylation of a 1:1 mixture of amide and ester.

We then proceeded to evaluate hypothesis **b** by computing the alkyl-intermediates and TSs for CO_2 insertion for the five substrates (**Table 1**). Interestingly, the energetically lowest-lying TS geometries all show an η^6-coordination mode of the substrate (**Figure 7A** and **Figure 11)**. CH···O=C interactions are observed with ester and amide as substrates, but are not possible for styrene-type substrates that lack a carbonyl group (for the latter, possible resonance structures are depicted in SI, Figure S6). It can also be seen that the CO_2 molecule does not interact with the metal center in any of the TSs. The conformational freedom of the CO_2 molecule implies that there potentially exists a large number of energetically close-lying TSs.

The analysis of the free energies shows that the ester has the lowest barrier (14.4 kcal/mol), whereas the highest activation energy was found for the amide (19.8 kcal/mol). This indicates that the barrier for CO_2 insertion could explain why esters are the preferred substrates and amides are unreactive.[5] The styrene and 1-methoxy-4-vinylbenzene have similar barriers of 16.7 and 16.4 kcal/mol, respectively, which is ~2 kcal/mol above the ester, in line with the lack of reactivity in experiment.[5] However, 1-(4-vinylphenyl)ethan-1-one has a relatively high CO_2 insertion barrier of 18.7 kcal/mol, in disagreement with the experimentally observed conversion. We cannot exclude that a lower CO_2 insertion TS exists for this particular substrate. Overall, the correlation for the four other substrate indicate that the CO_2 insertion barrier could explain the substrate preferences observed in rhodium-catalyzed hydrocarboxylation reactions.

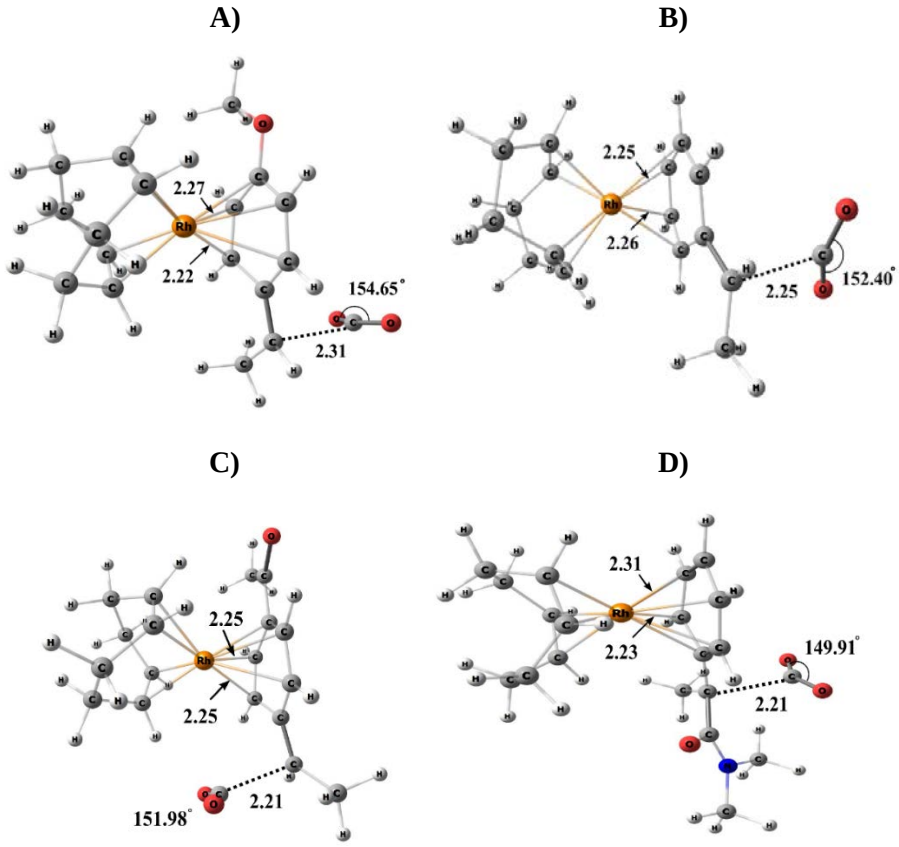

Figure 12. Optimized geometries for the CO_2 insertion TS for the substrates **A**) 1-methoxy-4-vinylbenzene, **B**) Styrene, **C**) 1-(4-vinylphenyl)ethan-1-one, **D**) *N*,*N*-dimethyl-2-phenylacrylamide. Distances are given in Angstrom.

CONCLUSIONS

The detailed mechanism of the highly regioselective rhodium-catalyzed hydrocarboxylation of styrene derivatives and α,β unsaturated carbonyl compounds with CO_2 was investigated using DFT theory, combined with experimental studies. The computational investigations reproduce the experimentally observed regioselectivity, and reveal that during the C-CO_2 bond formation step, the CO_2 molecule interacts with neither the rhodium complex nor the organozinc additive. This is in contrast to predictions on related reactions, which propose a CO_2-metal interaction.[8,9,10,11,12,13,14,20,21,22,23,24] In addition, we find that for the five studied substrates, the energetically lowest-lying TS geometries all show an unusual coordination mode of the substrate through the phenyl ring instead of through the nucleophilic carbon. Our calculations indicate that the rate-limiting CO_2 insertion barrier could provide an explanation to why esters are reactive and amides are unreactive. A possible poisoning effect of the amide was ruled out. Our experimental results are in agreement with the computationally computed mechanism. In addition, the experimental studies revealed two possible side reactions involving substrate dimerization or oxidative cleavage of the alkene, which were suppressed when the reaction was performed under a CO_2 atmosphere. The insights obtained here may be relevant for designing novel rhodium-catalyzed reactions for carbon-carbon bond formation with CO_2.

ASSOCIATED CONTENT

Supporting Information

The Supporting Information is available free of charge on the ACS Publications website:

- Optimized coordinates, which can be conveniently visualized with the Mercury program from the Cambridge Crystallographic Data Centre (XYZ file)
- Additional computational results as described in the text and experimental details (PDF)

AUTHOR INFORMATION

Corresponding Author: *kathrin.hopmann@uit.no

ACKNOWLEDGMENT

This work has been supported by the Research Council of Norway through a FRINATEK grant (No. 231706) and a Centre of Excellence Grant (No. 262695), by the Tromsø Research Foundation (No. TFS2016KHH), by Notur - The Norwegian Metacenter for Computational Science through grants of computer time (No. nn9330k and nn4654k), and by NordForsk (No. 85378) and the members of the *Nordic Consortium for CO_2 Conversion* (UiT – The Arctic University of Norway, Uppsala University, Stockholm University, KTH Royal Institute of Technology, Aarhus University, University of Oslo, University of Bergen, Helsinki University, University of Iceland).

REFERENCES

[1] Williams, C. M.; Johnson, J. B.; Rovis, T. Nickel-Catalyzed Reductive Carboxylation of Styrenes using CO_2. *J. Am. Chem. Soc.* **2008**, *130*, 14936-14937.

[2] Shirakawa, E.; Ikeda, D.; Masui, S.; Yoshida, M.; Hayashi, T. Iron–Copper Cooperative Catalysis in the Reactions of Alkyl Grignard Reagents: Exchange Reaction with Alkenes and Carbometalation of Alkynes. *J. Am. Chem. Soc.* **2012**, *134*, 272-279.

[3] Greenalgh, M. D.; Thomas, S. P. Iron-Catalyzed, Highly Regioselective Synthesis of α-Aryl Carboxylic Acids from Styrene Derivatives and CO_2. *J. Am. Chem. Soc.* **2012**, *134*, 11900-11903.

[4] Shao, P.; Wang, S.; Chen, C.; Xi, C. Cp2TiCl2-Catalyzed Regioselective Hydrocarboxylation of Alkenes with CO_2. *Org. Lett.* **2016**, *18*, 2050-2053.

[5] Kawashima, S.; Aikawa, K.; Mikami, K. Rhodium-Catalyzed Hydrocarboxylation of Olefins with Carbon Dioxide. *Eur. J. Org. Chem.* **2016**, 3166-3170.

[6] Murata, K.; Numasawa, N.; Shimomaki, K.; Takaya, J.; Iwasawa, N. Construction of a visible light-driven hydrocarboxylation cycle of alkenes by the combined use of Rh(I) and photoredox catalysts. *Chem. Commun.* **2017**, *53*, 3098-3101.

[7] Fan, T; Chen, X.; Lin, Z. Theoretical studies of reactions of carbon dioxide mediated and catalysed by transition metal complexes. *Chem. Commun.* **2012**, *48*, 10808-10828.

[8] Ren, Q.; Wu, N.; Ying, C.; Fang, J. DFT Study of the Mechanisms of Iron-Catalyzed Regioselective Synthesis of α-Aryl Carboxylic Acids from Styrene Derivatives and CO_2. *Organometallics*, **2016**, *35*, 3932–3938.

[9] Ostapowicz, T. G.; Hölscher, M.; Leitner, W. Catalytic Hydrocarboxylation of Olefins with CO_2 and H_2 -a DFT Computational Analysis. *Eur. J. Inorg. Chem.* **2012**, 5632–5641.

[10] Yuan, R.; Lin, Z. Computational Insight into the Mechanism of Nickel-Catalyzed Reductive Carboxylation of Styrenes using CO_2. *Organometallics* **2014**, *33*, 7147−7156.

[11] Vummaleti, S. V. C.; Talarico, G.; Nolan, S. P.; Cavallo, L.; Poater, A. How easy is CO2 fixation by M–C bond containing complexes (M = Cu, Ni, Co, Rh, Ir)? *Org. Chem. Front*. **2016**, *3*, 19–23.

[12] Lv,X.; Wu, Y.-B.; Lu, G. Computational exploration of ligand effects in copper-catalyzed boracarboxylation of styrene with CO_2. *Catal. Sci. Technol.* **2017**, *7*, 5049-5054.

[13] Fan, T.; Sheong, F. K.; Lin, Z. DFT Studies on Copper-Catalyzed Hydrocarboxylation of Alkynes Using CO_2 and Hydrosilanes. *Organometallics* **2013**, *32*, 5224−5230.

[14] Wang, Q.; Jia, J.-F.; Guo, C.-H.; Wu, H.-S. Mechanistic investigation of Cu(I)-mediated three-component domino reaction of asymmetrical alkynes with carbon dioxide: Theoretical rationale for the regioselectivity. *J. Organomet. Chem.* **2013**, *748*, 84-88.

[15] Dang, L.; Lin, Z.; Marder, T. B. DFT Studies on the Carboxylation of Arylboronate Esters with CO_2 Catalyzed by Copper(I) Complexes. *Organometallics* **2010**, *29*, 917–927.

[16] Sayyed, F. B.; Tsuji, Y.; Sakaki, S. The crucial role of a Ni(I) intermediate in Ni-catalyzed carboxylation of aryl chloride with CO_2: a theoretical study. *Chem. Commun.* **2013**, *49*, 10715-10717.

[17] Sayyed, F. B.; Sakaki, S. The crucial roles of $MgCl_2$ as a non-innocent additive in the Ni-catalyzed carboxylation of benzyl halide with CO_2. *Chem. Commun.* **2014**, *50*, 13026-13029.

[18] Graham, D. C.; Mitchell, C.; Bruce, M. I.; Metha, G. F.; Bowie, J. H.; Buntine, M. A. Production of Acrylic Acid through Nickel-Mediated Coupling of Ethylene and Carbon Dioxide—A DFT Study. O*rganometallics* **2007**, *26*, 6784-6792.

[19] Plessow, P.N.; Schäfer, A.; Limbach, M.; Hofmann, P. Acrylate Formation from CO2 and Ethylene Mediated by Nickel Complexes: A Theoretical Study. *Organometallics* **2014**, *33*, 3657–3668.

[20] Graham, D. C.; Bruce, M. I.; Metha, G.F.; Bowie, J.H.; Buntine, M.A. Regioselective control of the nickel-mediated coupling of acetylene and carbon dioxide – A DFT study. *J. Organomet. Chem.* **2008**, *693*, 2703–2710.

[21] Ostapowicz, T. G.; Hölscher, M.; Leitner, W. CO_2 Insertion into Metal-Carbon Bonds: A Computational Study of Rh(I) Pincer Complexes. *Chem. Eur. J.* **2011**, *17*, 10329 – 10338.

[22] Qin, H.; Han, J.; Hao, J.; Kantchev, E. B. Computational and experimental comparison of diphosphane and diene ligands in the Rh-catalysed carboxylation of organoboron compounds with CO_2. *Green Chem.* **2014**, *16*, 3224-3229.

[23] Obst, M.; Pavlovic, Lj.; Hopmann, K. H. Carbon-Carbon Bonds with CO_2: Insights from Computational Studies, *J. Organomet. Chem., In Press.*

[24] Lv, X.; Zhang, L.; Sun, B.; Li, Z.; Wu, Y.-B., Lu, G. Computational studies on the Rh-catalyzed carboxylation of a C(sp2)–H bond using CO_2. *Catal. Sci. Technol.* **2017**, *7*, 3539-3545.

[25] Schmeier, T. J.; Hazari, N.; Incarvito, C. D.; Raskatov, J. A. Exploring the reactions of CO_2 with PCP supported nickel complexes. *Chem. Commun.* **2011**, *47*, 1824-1826.

[26] Canepa G.; Brandt C.D.; Iig K.; Wolf J.; Werner H.; Exploring the reactions of CO_2 with PCP supported nickel complexes. *Chem. Eur. J.* **2003**, *9*, 2502-2515.

[27]Nolte M.J.; Gafner G.; Haines L.M.; An Example of the Co-ordination of the Tetraphenylboron Anion to a Transition Metal through an Arene Ring. *J. Chem. Soc, Chem.Commun*. **1969**, 1406-1407.

[28]Shao L.; Geib S.J.; Badger P.D.; Cooper J.N.; [2 + 2] Cross Coupling of Benzene and Tropylium Ligands in Reductively Activated Piano Stool Complexes of Mn, Cr, and W. *J. Am. Chem. Soc.* **2002**, *124*, 14812-14813.

[29]Doux M; Ricard L.; Mathey F.; Le Floch P.; Mezailles N.; Synthesis and Reactivity of the First η^6-Rhodium(I) and η^6-Iridium(I)Complexes of 2,6-Bis(trimethylsilyl)phosphinines *Eur. J. Inorg. Chem*, **2003**, 687-698.

[30] Gaussian 09, Revision D.01, Frisch, M. J.; Trucks, G. W.; Schlegel, H. B.; Scuseria, G. E.; Robb, M. A.; Cheeseman, J. R.; Scalmani, G.; Barone, V.; Mennucci, B.; Petersson, G. A.; Nakatsuji, H.; Caricato, M.; Li, X.; Hratchian, H. P.; Izmaylov, A. F.; Bloino, J.; Zheng, G.; Sonnenberg, J. L.; Hada, M.; Ehara, M.; Toyota, K.; Fukuda, R.; Hasegawa, J.; Ishida, M.; Nakajima, T.; Honda, Y.; Kitao, O.; Nakai, H.; Vreven, T.; Montgomery, J. A., Jr.; Peralta, J. E.; Ogliaro, F.; Bearpark, M.; Heyd, J. J.; Brothers, E.; Kudin, K. N.; Staroverov, V. N.; Kobayashi, R.; Normand, J.; Raghavachari, K.; Rendell, A.; Burant, J. C.; Iyengar, S. S.; Tomasi, J.; Cossi, M.; Rega, N.; Millam, J. M.; Klene, M.; Knox, J. E.; Cross, J. B.; Bakken, V.; Adamo, C.; Jaramillo, J.; Gomperts, R.; Stratmann, R. E.; Yazyev, O.; Austin, A. J.; Cammi, R.; Pomelli, C.; Ochterski, J. W.; Martin, R. L.; Morokuma, K.; Zakrzewski, V. G.; Voth, G. A.; Salvador, P.; Dannenberg, J. J.; Dapprich, S.; Daniels, A. D.; Farkas, Ö.; Foresman, J. B.; Ortiz, J. V.; Cioslowski, J.; Fox, D. J. Gaussian, Inc., Wallingford CT, **2009**.

[31] (a) Becke, A. D. A Density-fnnctional exchange-energy approximation with correct asymptotic behavior. *Phys. Rev*. **1988**, *38*, 3098-3100, (b) Lee, C.; Yang, W.; Parr, R.G., Development of the Colle-Salvetti correlation-energy formula into a functional of the electron density. *Phys. Rev. B* **1988**, *37*, 785-789.

[32] Grimme, S. Semiempirical GGA-Type Density Functional Constructedwith a Long-Range Dispersion Correction. *J. Comput. Chem.* **2006**, *27*, 1787-1799.

[33] (a) Tomasi, J.; Mennucci, B.; Cammi, R. Quantum Mechanical Continuum Solvation Models. *Chem. Rev.* **2005**, *105*, 2999-3093, (b) Tomasi, J.; Mennucci, B.; Cancès E. The IEF version of the PCM solvation method: an overview of a new method addressed to study molecular solutes at the QM ab initio level. *J. Mol. Struct.: THEOCHEM* **1999**, *464*, 211-216, (c) Cancès, E.; Mennucci, B.; Tomasi, J. A new integral equation formalism for the polarizable continuum model: Theoretical background and applications to isotropic and anisotropic
dielectrics. *J. Chem. Phys.* **1997**, *107*, 3032-3041.

[34] Hopmann, K. H. How Accurate is DFT for Iridium-Mediated Chemistry? *Organometallics* **2016**, *35*, 3795–3807.

[35] Ehlers, A.W.; Böhme, M.; Dapprich, S.; Gobbi, A.; Höllwarth, A.; Jonas, V.; Köhler, K. F.; Stegmann, R.; Veldkamp A.; Frenking, G.; A set of f-

polarization functions for pseudo-potential basis sets of the transition metals SC-Cu, Y-Ag and La-Au. *Chme. Phys. Lett.* **1993**, *208*, 111-114.
[36] (a) Boys, S.F.; Bernardi, F. The calculation of small molecular interactions by the differences of separate total energies. Some procedures with reduced errors. *Mol. Phys.* **1970**, *19*, 553-566, (b) Simon, S.; Duran, M.; Dannenberg, J. J., How does basis set superposition error change the potential surfaces for hydrogen-bonded dimers? *J. Chem. Phys.* **1996**, *105*, 11024-11031.
[37] Cramer, C.J. Essentials of Compuational Chemistry: Theories and models; *John Wiley & Soons Ltd*, **2004**, 378.
[38] Throughout the text, Rh-Alkyl refers to the alkyl formed from the alkene substrate. The rhodium-ethyl complex is referred to as Rh-Ethyl.
[39] Catellani M ;Mealli.C ;Motti E; Paoli P; Perez-Carreno E.; Pregosin P.S Palladium-Arene Interactions in Catalytic Intermediates: An Experimental and Theoretical Investigation of the Soft Rearrangement between η^1 and η^2 Coordination Modes . *J. Am. Chem. Soc*. **2002**, *124*, 4336-4346.
[40] Del Rosal, I., Maron, L.; Poteau, R.; Jolibois, F. DFT calculations of 1H and 13C NMR chemical shifts in transition metal hydrides. *Dalton Trans.* **2008**, *30*, 3959-3970.
[41] Kumaraswamy, G.; D. Rambabu, Hydroxy-rhodium(I) catalyzed regioselective Michael addition of cyclic enones. *Tetrahedron Lett.* **2012**, *53*, 1042-1044.
[42] Bönnemann, H., Rhodium-Catalyzed C,C-Double Bond Cleavage by Molecular Oxygen. *Helvetica Chimica Acta* **1983**, *66*, 177-184.

TOC